



**EUROfusion**

WPJET2-CPR(17) 16972

Y Hatano et al.

**Tritium Analysis of Divertor Tiles Used  
in JET ITER-like Wall Campaigns by  
Means of Beta-ray Induced X-ray  
Spectrometry**

Preprint of Paper to be submitted for publication in Proceeding of  
16th International Conference on Plasma-Facing Materials and  
Components for Fusion Applications



This work has been carried out within the framework of the EUROfusion Consortium and has received funding from the Euratom research and training programme 2014-2018 under grant agreement No 633053. The views and opinions expressed herein do not necessarily reflect those of the European Commission.

This document is intended for publication in the open literature. It is made available on the clear understanding that it may not be further circulated and extracts or references may not be published prior to publication of the original when applicable, or without the consent of the Publications Officer, EUROfusion Programme Management Unit, Culham Science Centre, Abingdon, Oxon, OX14 3DB, UK or e-mail [Publications.Officer@euro-fusion.org](mailto:Publications.Officer@euro-fusion.org)

Enquiries about Copyright and reproduction should be addressed to the Publications Officer, EUROfusion Programme Management Unit, Culham Science Centre, Abingdon, Oxon, OX14 3DB, UK or e-mail [Publications.Officer@euro-fusion.org](mailto:Publications.Officer@euro-fusion.org)

The contents of this preprint and all other EUROfusion Preprints, Reports and Conference Papers are available to view online free at <http://www.euro-fusionscipub.org>. This site has full search facilities and e-mail alert options. In the JET specific papers the diagrams contained within the PDFs on this site are hyperlinked

## **Tritium Analysis of Divertor Tiles Used in JET ITER-Like Wall Campaigns by Means of $\beta$ -ray Induced X-ray Spectrometry**

Y. Hatano<sup>a\*</sup>, K. Yumizuru<sup>a</sup>, S. Koivuranta<sup>b</sup>, J. Likonen<sup>b</sup>, M. Hara<sup>a</sup>, M. Matsuyama<sup>a</sup>,  
S. Masuzaki<sup>c</sup>, M. Tokitani<sup>c</sup>, N. Asakura<sup>d</sup>, K. Isobe<sup>d</sup>, T. Hayashi<sup>d</sup>, A. Baron-Wiechec<sup>e</sup>,  
A. Widdowson<sup>e</sup> and JET contributors\*\*

EUROfusion Consortium, JET, Culham Science Centre, Abingdon, OX14 3DB, UK

<sup>a</sup>Hydrogen Isotope Research Center, University of Toyama, Toyama 930-8555, Japan

<sup>b</sup>VTT Technical Research Centre of Finland, PO Box 1000, FI-02044 VTT, Finland

<sup>c</sup>National Institute for Fusion Science, Toki 509-5292, Japan

<sup>d</sup>National Institutes for Quantum and Radiological Science and Technology,  
Rokkasho 039-3212, Japan

<sup>e</sup>Culham Centre for Fusion Energy, Culham Science Centre, Abingdon, OX14 3DB, UK

\*Corresponding Author

Tel.: +81 76 445 6928; fax: +81 76 445 6931.

E-mail address: hatano@ctg.u-toyama.ac.jp (Y. Hatano)

\*\*See the author list of “Overview of the JET results in support to ITER” by X. Litaudon et al.  
to be published in Nuclear Fusion Special issue: overview and summary reports from the 26th  
Fusion Energy Conference (Kyoto, Japan, 17-22 October 2016)

PACS number

28.52.Fa (Fusion reactors, Materials)

28.52.Lf (Fusion reactors, Components and instrumentation)

52.55.Rk (Magnetic confinement and equilibrium, Power exhaust; divertors)

23.40.-s ( $\beta$  decay; double  $\beta$  decay; electron and muon capture)

29.40.-n (Radiation detectors)

## Abstract

Energy spectra of  $\beta$ -ray induced X-rays from divertor tiles used in JET ITER-like wall campaigns were measured to examine T penetration into W layers. The penetration depth of T evaluated from the intensity ratio of W  $L\alpha$  X-rays to W  $M\alpha$  X-rays showed clear correlation with poloidal position; the penetration depth at the upper divertor region reached several micrometers, while that at the lower divertor region was less than 500 nm. The deep penetration at the upper part was ascribed to the implantation of high energy T produced by DD fusion reactions. The poloidal distribution of total X-ray intensity indicated higher T retention in the inboard side than the outboard side.

## 1. Introduction

JET performed ITER-like wall (JET-ILW) campaigns with main chamber walls made of Be and divertor regions comprised of bulk tungsten (W) and W-coated carbon-fiber composite (CFC) tiles. A part of tiles used were retrieved after JET-ILW campaigns in 2011–2012 (ILW-1) and 2013–2014 (ILW-2) for post-mortem analysis [1]. Heinola et al. [2,3] examined deuterium (D) retention in the tiles retrieved after ILW-1 using nuclear reaction analysis (NRA), secondary ion mass spectrometry (SIMS) and thermal desorption spectrometry (TDS). They reported that the higher D retention was observed at the locations with thick deposition, and the highest retention was found at the top surface of inner divertor [3]. Heinola et al. [3] and Likonen et al. [4] also measured retention of tritium (T) produced by DD fusion reactions using TDS [3] and reported that T distribution was more uniform than that of D. They observed two desorption peaks at 700–800 °C and lower temperatures [3,4]. The high temperature desorption peak was ascribed to implantation of high energy T produced by the fusion reactions ( $D + D \rightarrow 1.01 \text{ MeV T} + 3.03 \text{ MeV p}$ ). Hatano et al. [5,6] examined T distributions in divertor tiles retrieved after ILW-1 by measuring  $\beta$ -rays from T using an imaging plate (IP) technique. Because of low energy of  $\beta$ -rays from T ( $\leq 18.6 \text{ keV}$ ), the escape depth of  $\beta$ -rays is small ( $\sim 3 \text{ }\mu\text{m}$  in Be and  $\sim 0.3 \text{ }\mu\text{m}$  in W). Therefore, this technique is sensitive to T on/near the surfaces of tiles. The clear correlation between T concentration and thickness of deposition layers was observed in the IP measurements. However, neither of TDS and IP techniques provided direct information on depth profiles of T.

In this study, the penetration depth of T in W layers was examined by  $\beta$ -ray induced X-ray spectrometry (BIXS) for divertor tiles retrieved after ILW-2. The energy spectra of X-rays induced by  $\beta$ -rays from T were measured using a conventional silicon drift detector (SDD) with 8  $\mu\text{m}$ -thick Be window. The major characteristic X-rays emitted by W in the energy region below 18.6 keV are W  $M\alpha$  (1.775 keV) and W  $L\alpha$  (8.398 keV) X-rays.

Because the attenuation of W  $L\alpha$  X-rays in W is far weaker than that of W  $M\alpha$  X-rays, the intensity ratio of W  $L\alpha$  X-rays to W  $M\alpha$  X-rays,  $I_{W-L\alpha}/I_{W-M\alpha}$ , increases with increasing penetration depth of T, as discussed in [7]. From this correlation, one can roughly evaluate the penetration depth of T. X-ray spectra from several selected positions on the divertor tiles retrieved after ILW-1 were also measured using a SDD with an ultra-thin window (70 nm-thick  $\text{Si}_3\text{N}_4$ ) to examine the influence of Be on X-ray spectra by detecting Be  $K\alpha$  X-rays (0.1085 keV).

## 2. Experimental procedures

The disk samples (17 mm diameter) cut from the divertor tiles retrieved after ILW-2 were examined using the SDD with 8  $\mu\text{m}$ -thick Be window (AMPTEK X-123SDD) in VTT Technical Research Center of Finland. The positions analyzed are shown in Fig. 1 by blue numbers together with the cross-sectional view of JET divertor region. Black numbers indicate tile numbers and s-coordinate which is equivalent to the distance along the tile surfaces in mm. The W-coated tiles examined were Tiles 0 (Tile code: HFGC Mod13 RH, 2010–2014 and Mod14 LH, 2012–2014), 1 (14ING1C, 2012–2014), 3 (2IWG3A, 2010–2014), 6 (14BNG6D, 2010–2014), 7 (14ONG7A, 2010–2014) and 8 (14ONG8A, 2010–2014). The surface of Tile 4 examined was covered by Mo layer and not W layer. Some tiles were used in both ILW-1 and ILW-2 (2010–2014), and others were exposed to the plasma solely in ILW-2 (2012–2014). The measurements were performed under Ar gas atmosphere (0.1 MPa). The distance between sample surface and detector window was  $\sim 1$  mm. The measurement time was 24–52 hours. The 8  $\mu\text{m}$ -thick Be window has negligible transmittance in the energy region below 0.6 keV. Hence the detection of characteristic X-rays of low-Z elements such as Be, C and O is impossible with this window.

The correlation between  $I_{W-L\alpha}/I_{W-M\alpha}$  and the penetration depth of T was evaluated by Monte Carlo simulation using Geant4 tool kit [8–10]. Procedures of simulation were similar

to those given in [11]. The accuracy of evaluation was examined using a reference W sample. A plate of W was irradiated with 20 MeV W ions to 0.5 displacement per atom to induce defects acting as traps against hydrogen isotopes. The depth profiles of D measured using NRA after exposing the sample to D<sub>2</sub> gas at 673 K showed that D penetrated almost uniformly up to a depth of 2 μm being close to the range of 20 MeV W ions in W (see Fig. 4 in [12]). The reference sample was prepared by exposing the irradiated W plate to D-5%T mixture gas at 673 K. The value of  $I_{W-L\alpha}/I_{W-M\alpha}$  was obtained by the simulation to be 0.114 by assuming uniform T penetration up to a depth of 2 μm. This value agreed well with  $I_{W-L\alpha}/I_{W-M\alpha}$  derived from the measured X-ray spectrum, 0.113.

The analysis using the SDD with 70 nm-thick Si<sub>3</sub>N<sub>4</sub> window (AMPTEK C2 window) was performed in International Fusion Energy Research Centre (IFERC), National Institutes for Quantum and Radiological Science and Technology (QST). In contrast to a conventional Be window, this type of window has transmittance at X-ray energy below 0.6 keV [13]. The measurements were performed at reduced pressure (1 Pa) to avoid attenuation of low energy X-rays in air. On the other hand, direct incidence of β-rays to the SDD and consequent generation of bremsstrahlung X-rays in the detector occurred at this pressure. To reduce the flux of β-rays to the SDD, a sample surface was covered by very thin (1.2 μm thickness) film of polyphenylene sulfide. Sample disks examined were cut from the poloidal positions 10 and 5 of Tile 1 (14ING1C), 10 of Tile 4 (14BNG4D), 2 and 9 of Tile 6 (2BNG6C), 8 of Tile 7 (2ONG7A) and 10 of Tile 8 (2ONG8B) retrieved after ILW-1.

### 3. Results and discussion

Typical examples of X-ray spectra are given in Fig. 2 in which (a)–(c) were measured with the 8 μm-thick Be window and (d) was acquired with the ultra-thin window. Fig. 2 (a) shows X-ray spectrum of the sample from the horizontal part (apron) of Tile 1 (position 12). The characteristics of this spectrum are strong bremsstrahlung X-rays at 1–4



keV, weak W  $M\alpha$  and very weak W  $L\alpha$  X-rays in comparison with Ar  $K\alpha$  X-rays, and appearance of Cr and Ni  $K\alpha$  X-rays. The characteristic X-rays of Ar is generated by  $\beta$ -rays from T present at the surface and subsurface layers within the escape depth of  $\beta$ -rays. Similar spectra were obtained for positions 5–1 of Tile 0 and position 10 of Tile 1. Fe  $K\alpha$  peak was also observed in the case of Tile 0. Fig. 2 (b) shows the spectrum for the upper vertical part of Tile 1 (position 9). A large peak of W  $M\alpha$  X-rays was observed together with intense W  $L\alpha$  X-rays and bremsstrahlung X-rays at 4–10 keV. Similar spectra were observed for other positions in the upper vertical part of Tile 1, and Tile 8. A typical spectrum for lower vertical tiles and floor tiles is given in Fig. 2 (c) (position 5 of Tile 3). The intensity of W  $L\alpha$  X-rays is very weak in comparison with that of W  $M\alpha$  X-rays. In addition, the intensity of bremsstrahlung X-rays monotonously decreases with increasing energy. Similar spectra were observed for other positions of Tile 3, and Tiles 6 and 7. Fig. 2 (d) shows the spectrum from the apron of Tile 1 (position 10). A intense peak of Be  $K\alpha$  X-rays was observed. The strong bremsstrahlung X-rays was due to the direct incidence of  $\beta$ -rays to the SDD, as mentioned above. No noticeable peak of Be  $K\alpha$  X-rays was observed for other samples except the sample from position 5, Tile 1 showing a small Be  $K\alpha$  peak. The peak of Mo  $L\alpha$  X-rays was observed for Tile 4, as expected (not shown).

The observations of intense Be  $K\alpha$  peak at the apron of Tile 1 (Fig. 2 (d)) and the  $K\alpha$  peaks of Cr, Fe and Ni at Tile 0 and the apron of Tile 1 (Fig. 2 (a)) agree well with the formation of thick deposition layers of Be and other impurities reported in [14]. The strong bremsstrahlung X-rays relative to W  $M\alpha$  X-rays in Fig. 2 (a) is explained by the generation of bremsstrahlung X-rays by  $\beta$ -rays from T present in thick Be deposition layers. As reported in [5], the IP measurements showed that T concentration in the deposition layers formed on the apron of Tile 1 retrieved after ILW-1 reached  $\sim 10\text{--}20 \text{ MBq cm}^{-3}$ .

The difference between Figs. 2 (b) and (c) indicate that the value of  $I_{W-L\alpha}/I_{W-M\alpha}$  varies with poloidal position. The values of  $I_{W-L\alpha}/I_{W-M\alpha}$  are plotted in Fig. 3 against

s-coordinate. In this figure, the values for Tile 0 and the apron of Tile 1 are not plotted due to severe impurity depositions, and those for Tile 4 are also omitted because of the presence of Mo layer on the surface. Clear correlation was observed between  $I_{W-L\alpha}/I_{W-M\alpha}$  and poloidal positions, and  $I_{W-L\alpha}/I_{W-M\alpha}$  took high values at the upper part of the divertor region and decreased with increasing distance from the core plasma. The values of  $I_{W-L\alpha}/I_{W-M\alpha}$  was 0.1–0.18 at the upper part and 0.01–0.03 at the bottom part of the divertor region.

The simulation using Geant4 showed  $I_{W-L\alpha}/I_{W-M\alpha} = 0.060$  at T penetration depth of 0.5  $\mu\text{m}$ , 0.076 at 1.0  $\mu\text{m}$ , 0.104 at 1.5  $\mu\text{m}$ , 0.114 at 2.0  $\mu\text{m}$ , 0.160 at 3.0  $\mu\text{m}$  and 0.187 at 4.0  $\mu\text{m}$ . The uniform distribution of T up to the indicated penetration depths was assumed in the simulation for simplicity. According to the simulation using SRIM program [15], the range of 1.01 MeV T in W is 4.6  $\mu\text{m}$  at the normal incidence. The values of  $I_{W-L\alpha}/I_{W-M\alpha}$  observed at the upper part of divertor region (0.1–0.18) correspond to the penetration depth of T from  $\sim 1.5$ –4.0  $\mu\text{m}$ ; the maximum penetration depth thus evaluated was close to the range of 1.01 MeV T in W. The penetration depth at the bottom part appears to be far less than 500 nm. The mechanisms underlying the variation of penetration depth may be understood by comparing the results of the present study with those of ASCOT Monte Carlo simulations [3]. The observations in this study support the statement of Heinola et al. [3] on the implantation of energetic T into the tiles.

The values of total X-ray counts are plotted against s-coordinate in Fig. 4 together with those of T retention measured by Heinola et al. [3] using a technique of TDS. X-ray counts for Tile 0, the apron of Tile 1 and Tile 4 are not shown in this figure because the efficiency of X-ray generation by  $\beta$ -rays in Be and Mo is different from that in W. The total X-ray intensity in the inboard side is higher than that in the outboard side, and the maximum intensity was observed for the upper vertical part of Tile 1. Although the total X-ray intensity is not simply proportional to T retention, this observation suggests that the inboard tiles retained more T than the outboard tiles. Detailed comparison between BIXS data and TDS

data is difficult at this moment because the values for upper vertical part of Tile 1 are missing in the data set reported in [3]. Nevertheless, available data show no serious disagreement.

#### 4. Conclusions

The energy spectra of  $\beta$ -ray induced X-rays from divertor tiles retrieved from JET after ILW-2 and ILW-1 were measured to examine T penetration into W layers. Clear correlation was observed between penetration depth of T and poloidal position; the penetration depth at the upper divertor region reached several micrometers, while that at the lower divertor region was less than 500 nm. The deep penetration at the upper part was ascribed to the implantation of high energy T produced by DD fusion reactions. The poloidal distribution of X-ray intensity indicated higher T retention in the inboard side than the outboard side.

#### Acknowledgements

This work has been carried out within the framework of the EUROfusion Consortium and has received funding from the Euratom research and training programme 2014-2018 under grant agreement No 633053. The views and opinions expressed herein do not necessarily reflect those of the European Commission. The study was supported by JSPS KAKENHI Grant Number 26289353, QST under the Joint Work contract 26K276, as a part of Broader Approach activities, and the National Institute for Fusion Research (NIFS) as a part of PWI Collaboration. The authors express their sincere thanks to Dr. K. Sugiyama in Max-Planck Institut für Plasmaphysik for his kind help in the preparation and D measurements of the reference sample.

## References

- [1] Widdowson A *et al* 2017 Overview of the JET ITER-like wall divertor *Nucl. Mater. Energy* at press. (doi.org/10.1016/j.nme.2016.12.008)
- [2] Heinola K *et al* 2015 *J. Nucl. Mater.* **463** 961–965
- [3] Heinola K *et al* 2016 *Phys. Scr.* **T167** 014075
- [4] Likonen J *et al* 2016 *Phys. Scr.* **T167** 014074
- [5] Hatano Y *et al* 2015 *J. Nucl. Mater.* **463** 966–969
- [6] Hatano Y *et al* 2016 *Phys. Scr.* **T167** 014009
- [7] Matsuyama M *et al* 2002 *J. Nucl. Mater.* **307-311** 729-734
- [8] Agostinelli S *et al* 2003 *Nucl. Instrum. Meth. Phys. Res. A* **506** 250–303
- [9] Allison J *et al* 2006 *IEEE Trans. Nucl. Sci.* **53** 270–278
- [10] Allison J *et al* 2016 *Nucl. Instrum. Meth. Phys. Res. A* **835** 186–225
- [11] Hara M *et al* 2017 *Fusion Eng. Des.* **119** 12–16
- [12] Hatano Y *et al* 2013 *J. Nucl. Mater.* **438** S114–S119
- [13] <http://amptek.com/products/c-series-low-energy-x-ray-windows/>
- [14] Baron-Wiechec A *et al* 2015 *J. Nucl. Mater.* **463** 157–161
- [15] Ziegler J F, <http://www.srim.org/>

## Figure captions

Fig. 1 Cross-sectional view of JET divertor region and poloidal positions of samples (blue numbers) in the tiles retrieved after ILW-2. White letters indicate tile numbers, and red numbers are s-coordinates which are the distance along the tile surface in mm [1].

Fig. 2 Typical X-ray spectra from JET divertor tiles; (a) position 12, Tile 1, (b) position 9, Tile 1, (c) position 5, Tile 3 and (d) position 10, Tile 1. (a)–(c) were measured for the tiles retrieved after ILW-2 under Ar gas atmosphere using SDD with 8  $\mu\text{m}$ -thick Be window having no transmission in energy region below 0.6 keV. (d) was acquired using SDD with 70 nm-thick  $\text{Si}_3\text{N}_4$  window at reduced pressure (1 Pa) for the tile retrieved after ILW-1.

Fig. 3 Correlation between intensity ratio of W  $L\alpha$  X-rays to W  $M\alpha$  X-rays ( $I_{W-L\alpha}/I_{W-M\alpha}$ ) and poloidal positions (s-coordinate) in divertor region. Measurements were performed for the tiles retrieved after ILW-2 using SDD with Be window.

Fig. 4 Correlation between total X-ray counts and poloidal positions (s-coordinate) in divertor region. Measurements were performed for the tiles retrieved after ILW-2 using SDD with Be window. Black squares indicate T retention measured by Heinola et al [3] using TDS technique.

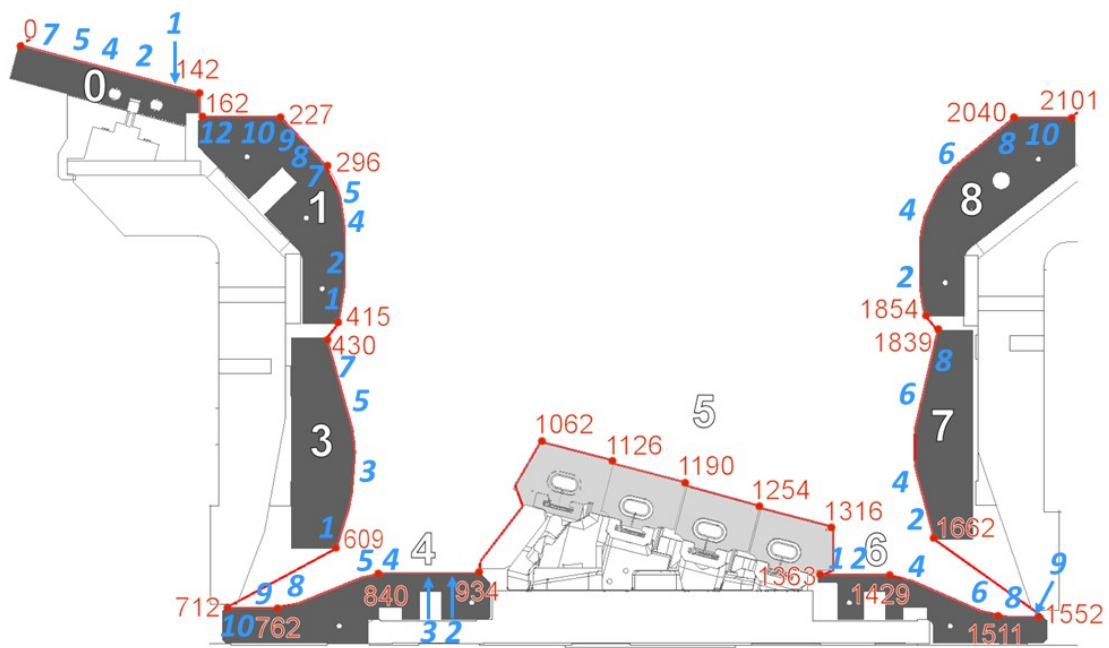


Fig. 1 Cross-sectional view of JET divertor region and poloidal positions of samples (blue numbers) in the tiles retrieved after ILW-2. White letters indicate tile numbers, and red numbers are s-coordinates which are the distance along the tile surface in mm [1].

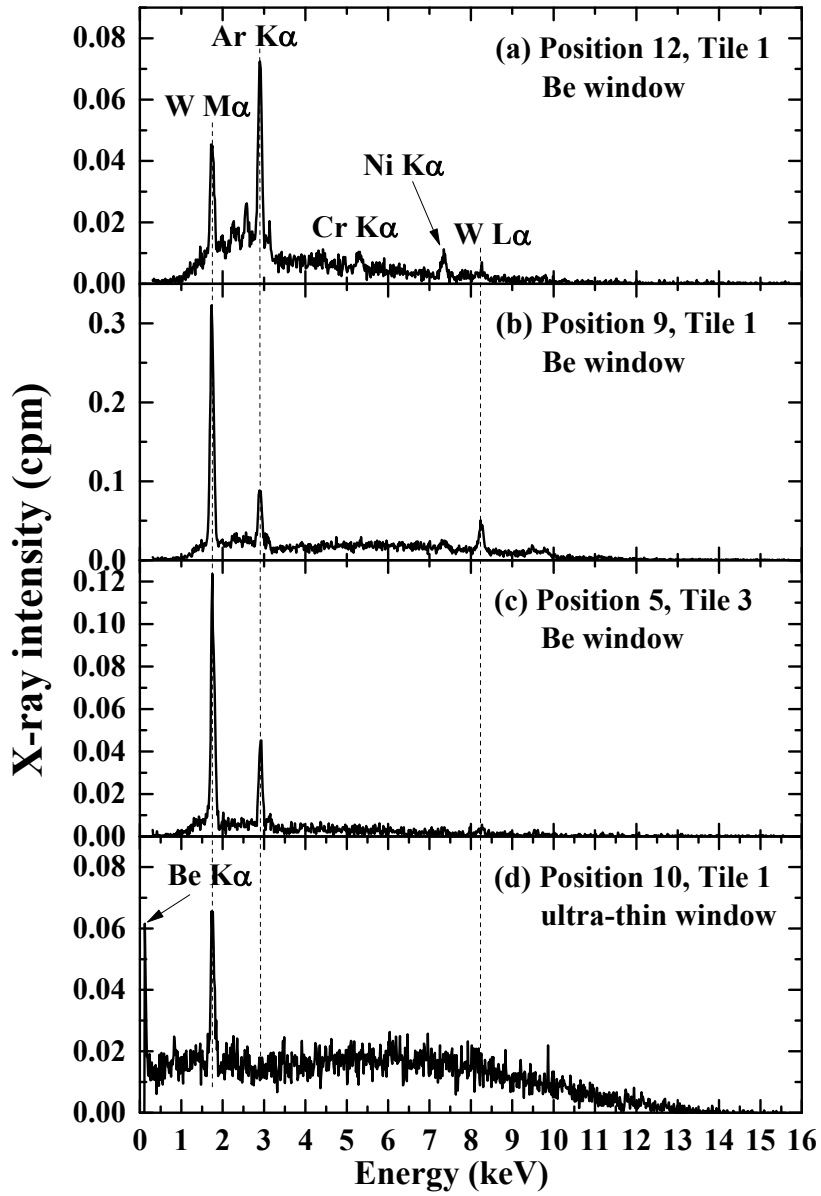


Fig. 2 Typical X-ray spectra from JET divertor tiles; (a) position 12, Tile 1, (b) position 9, Tile 1, (c) position 5, Tile 3 and (d) position 10, Tile 1. (a)–(c) were measured for the tiles retrieved after ILW-2 under Ar gas atmosphere using SDD with 8  $\mu$ m-thick Be window having no transmission in energy region below 0.6 keV. (d) was acquired using SDD with 70 nm-thick Si<sub>3</sub>N<sub>4</sub> window at reduced pressure (1 Pa) for the tile retrieved after ILW-1. (one column)

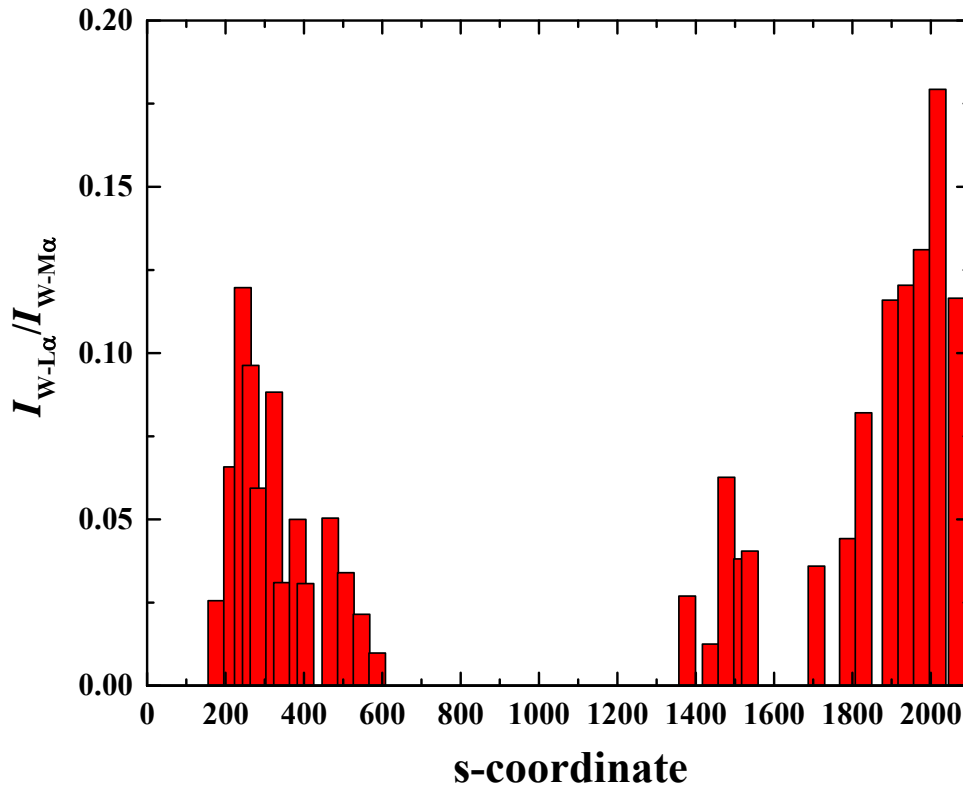


Fig. 3 Correlation between intensity ratio of W L $\alpha$  X-rays to W M $\alpha$  X-rays ( $I_{W-L\alpha}/I_{W-M\alpha}$ ) and poloidal positions (s-coordinate) in divertor region. Measurements were performed for the tiles retrieved after ILW-2 using SDD with Be window.

(one column)



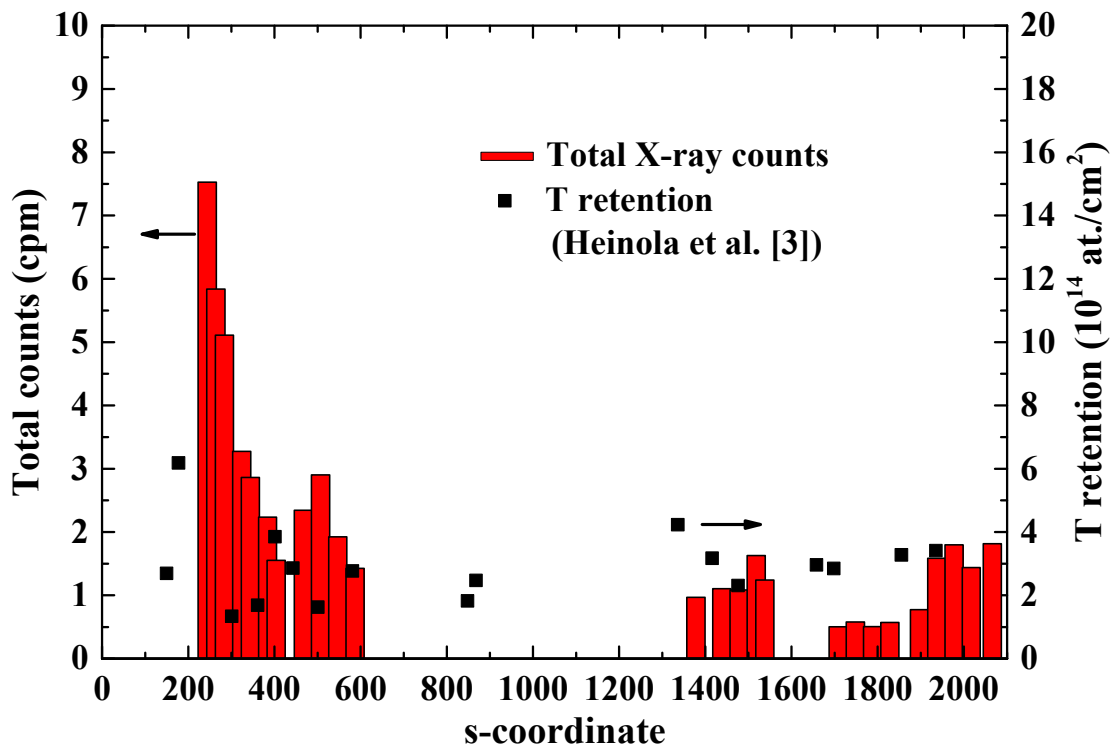


Fig. 4 Correlation between total X-ray counts and poloidal positions (s-coordinate) in divertor region. Measurements were performed for the tiles retrieved after ILW-2 using SDD with Be window. Black squares indicate T retention measured by Heinola et al [3] using TDS technique.

(one column)